www.czasopisma.pan.pl PAN POLSKA AKADEMIA NAUK www.journals.pan.pl

Arch. Metall. Mater. **64** (2019), 2, 597-601

DOI: 10.24425/amm.2019.127584

M.W. LEE*, J.K. LEE*, T.S. JANG*#

EFFECT OF PRE-SINTERING ON THE DIFFUSION TREATMENT OF HRE FOR COERCIVITY ENHANCEMENT OF A NdFeB SINTERED MAGNET

We investigated the effect of pre-sintering process on the penetration behavior of Dy in a NdFeB sintered magnet which was grain boundary diffusion treated with Cu/Al mixed Dy source. The pre-sintering of a magnet was performed at 900°C in vacuum and then the pre-sintered body was dipped in the solutions of DyH_2, DyH_2 + Cu, and DyH_2 + Al, respectively. The dipped pre-sintered body were then fully sintered 4 hours at 1060°C followed by a subsequent annealing. The pre-sintering apparently improved the diffusivity of Dy atoms. The penetration of Dy into the magnet extended almost to 2,000 μm from the surface, about four times deeper than that of the normally sintered and diffusion treated one, when the DyH_2 + Al solution was used as a Dy source. However, the resulting increase of coercivity was about 4 kOe, somewhat lower than that of the normally treated one, mostly due to excessive oxide formation that hindered to make a continuous Nd-rich grain boundary phase and a core-shell type structure.

Keywords: Grain boundary diffusion process (GBDP), NdFeB magnet, Coercivity, Pre-sintering

1. Introduction

The coercivity of NdFeB sintered magnets is known to be controlled by the mechanism based on reverse magnetic domain nucleation at the grain boundaries [1-3]. In order to obtain high coercivities over 25 kOe from the NdFeB sintered magnet, for high temperature application such as a traction motor in HEV or EV [4,5], certain amount of heavy rare-earth (HRE) elements, typically Dy is normally added to the magnetic alloy during the alloy preparation step so that the anisotropy field (H_A) of hard magnetic $Nd_2Fe_{14}B$ grains is increased by partial substitution of Nd with Dy to form $(Nd,Dy)_2Fe_{14}B$.

Since the coercivity of NdFeB sintered magnets is determined by the easiness of the nucleation of reverse magnetic domains at grain boundary area, it is possible to obtain high enough coercivity if H_A of the surface region of a hard magnetic grain is locally increased by concentrating Dy only around the grain, making the so-called core-shell type structure [6-8]. By realizing such core-shell type structure, one can not only reduce the usage of HRE but also minimize the reduction of magnetization, i.e., (BH)max, caused by the antiferromagnetic coupling between the HRE and Fe atoms.

The best way that has been developed so far to make the core-shell type structure is grain boundary diffusion process (GBDP), in which Dy is diffused into a magnet from the magnet surface along the reactive grain boundaries upon heating [6-8]. However, there is a certain limit in diffusion depth of the Dy atoms because the magnet used for this process is fully dense, resulting in relatively shallow penetration of the Dy atoms into the magnet and uneven magnetic properties depending on the distance from the magnet surface, especially when the magnet becomes thicker [9]. The magnetic properties of a GBDP magnet are then simply average values measured from entire volume of the magnet. In GBDP, therefore, it is also important to increase the penetration depth of HRE atoms effectively to secure more uniform core-shell type grains and stable magnetic properties.

A pre-sintering (PS) process, for which a magnet is sintered as a primary step below 900°C prior to fully dense sintering at a higher temperature could increase the penetration depth of HRE atoms by decreasing the density of the sintered body to 70 ~ 80%. In addition, Cu and Al also improve the diffusivity of HRE atoms by improving the wettability of Nd-rich grain boundary phase [10]. The solubility of Cu to $Nd_2Fe_{14}B$ phase is almost negligible whereas Al has some solubility to this main phase [1,3,10]. In this study, we adopted the pre-sintering process for the grain boundary diffusion process and investigated its effectiveness on the penetration behavior of Dy in a NdFeB sintered magnet which was diffusion treated with Cu/Al mixed Dy source.

2. Experimental

Magnetic powder with average particle size of 5 μm and a nominal composition of $Nd_{29.00}Dy_{3.00}Fe_{Bal.}B_{0.97}M_{2.39}$ (wt.%, M = Cu, Al, Co and Nb) was prepared in sequence of strip

* SUNMOON UNIVERSITY, DEPT. OF ADVANCED MATERIALS ENGINEERING, ASAN, CHUNGNAM 336-708, KOREA

Corresponding author: tsjang@sunmoon.ac.kr

casting, hydrogen decrepitation, and jet milling. To prepare a pre-sintered (PS) sample, the magnetic powder was uniaxially compacted under a magnetic field of 2.2 T and then sintered one hour at 900°C. A normal fully dense magnet sample was also prepared by sintering 4 hours at 1070°C for comparison. The solution for grain boundary diffusion (GBD) treatment was prepared by mixing the powders of DyH_2 (~2 μm), Cu (~1 μm), and Al(~1 μm) with absolute ethanol. Three kinds of solutions; DyH_2, DyH_2 + Al (1:1 w/w), and DyH_2 + Cu (1:1 w/w) of 50 wt% each, were prepared as Dy supplier for the treatment. Both the pre-sintered and the normally sintered bulk samples, cut into a size of 12.5 mm × 12.5 mm × 5 mm, were then immersed in the solution for 1min with applying ultrasonic vibration, and dried immediately by hot air. The Dy-source coated PS samples were sintered again for 4 hours at 1060°C for full densification and Dy diffusion. Finally, both the sintered PS samples and the Dy-source coated normal samples were annealed at 850°C and then 530°C for 2 hours each. All sintering and annealing were performed in vacuum (~10^{-5} Torr). Magnetic properties of the samples were measured using a B-H loop tracer (Magnet-Physik Permagraph C-300). Microstructural investigation was carried out using a scanning electron microscopy (SEM, JXA-8500F) and high resolution transmission electron microscopy (HRTEM, JEOL JEM 2100F). The distribution of Dy and other elements after GBD treatment was analyzed with EPMA (SHIMADZU EPMA-1720).

3. Results and discussion

Fig. 1(a) shows fracture surface of a bulk pre-sintered at 900°C for one hour. Because the bulk was not completely consolidated by liquid-phase sintering at this stage, many pores were found in triple junctions, yielding a density of 6.4 g/cm^3 which

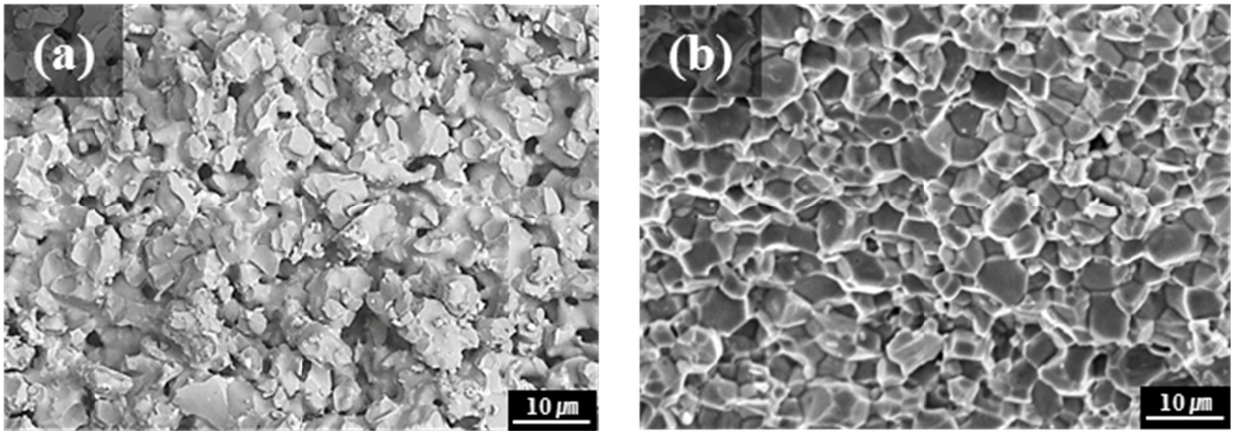

Fig. 1. SEM micrographs of magnet samples (a) after pre-sintered only at 900°C and (b) after fully sintered again at 1600°C for 4 hours

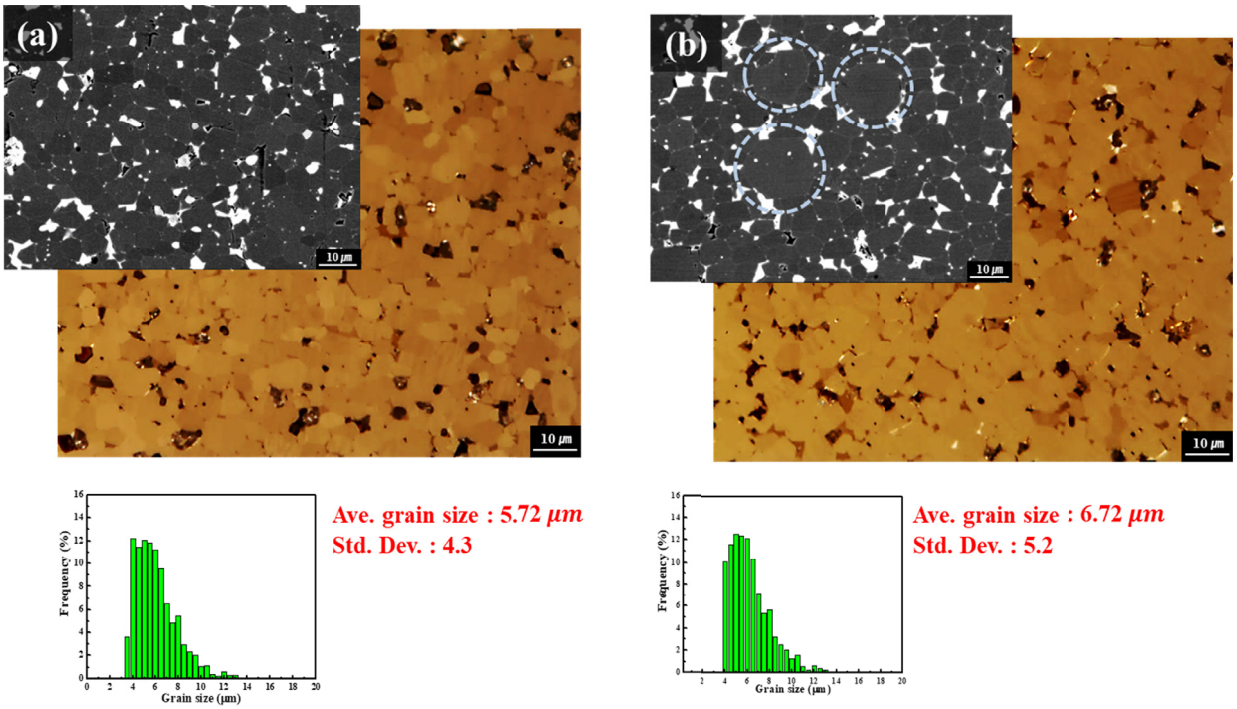

Fig. 2. SEM BSE images and comparison of grain configuration between (a) the normally sintered magnet and (b) the PS sintered one

is about 84% of that of a normally sintered bulk. (See Table 1) As shown in Fig. 1 (b), those pores were disappeared and the fracture surface was very similar to that of a normally sintered one when the pre-sintered body was sintered again 4 hours at 1060°C for full densification. Hereafter, we will call this two-step sintered body as a PS sintered body or magnet. The density of this PS sintered body was 7.48 g/cm^3, reached almost 98% of that of the normal full dense magnet.

While the normally sintered body revealed even distribution of hard magnetic grains with the average grain size of 5.72 μm, as shown in Fig. 2 (a), abnormal grain growth was occurred in the PS sintered one (circled area in Fig. 2 (b)), resulting in a larger average grain size (6.72 μm) and wider standard deviation (5.2 vs 4.3). Such abnormal grain growth may cause slight deviation of uniaxial magnetic alignment of the hard magnetic phase [11]. Along with lower density, this microstructural difference is largely responsible for the decrease in remanence (B_r) values in the PS sintered magnet, as revealed in Fig. 3, because B_r is proportional to the density and the degree of alignment of magnetic phase [11].

Fig. 3 shows demagnetization curves of the PS sintered GBDP magnets, and their magnetic properties and densities are summarized in Table 1. Magnetic properties of the normally sintered one are also listed in Table 1 for comparison. Together with the density, B_r of all PS sintered magnets were slightly lower than that of the normal one mainly due to the reason explained above. When the grain boundary diffusion treatment was carried out with Al mixed Dy source, the increase of the coercivity ($_iH_c$) was always higher (4.0 kOe) than that treated with Cu mixed source (3.2 kOe) as observed in elsewhere [10,12,13].

As can be seen in Fig. 4, the penetration depth of Dy was remarkably increased by adopting the pre-sintering process. While Dy reached to about 520 μm from the surface owing to the addition of Al in normally sintered GBDP magnet [10], it reached almost to 2,000 μm after adopting the PS step, about four times deeper than the former. However, the increase of $_iH_c$ by GBDP of the PS sintered magnet was smaller (4.0 kOe) than that obtained from the normally sintered GBDP magnet

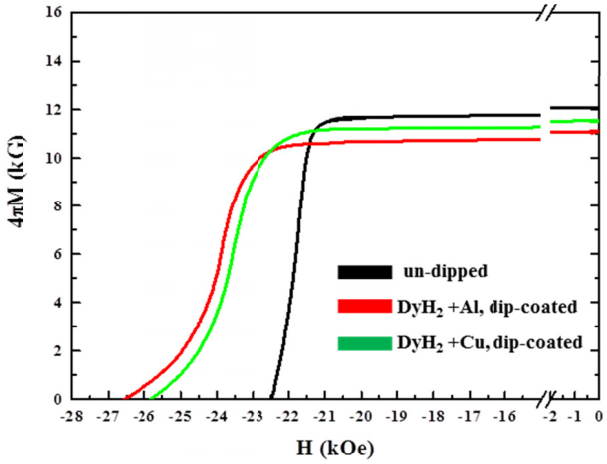

Fig. 3. Demagnetization curves of the grain boundary diffusion treated PS sintered magnets

TABLE 1

Magnetic properties and densities of the PS sintered and the normally sintered magnets.

Type	Conditions	B_r (kG)	$_iH_c$ (kOe)	Δ_iH_c (kOe)	(BH)max (MGOe)	Density (g/cm^3)
PS sintered	un-dipped	12.2	22.5	—	36.4	7.48
	DyH_2+Al dip-coated	11.0	26.5	4.0	29.6	7.46
	DyH_2+Cu dip-coated	11.5	25.7	3.2	32.4	7.46
Normally sintered	un-dipped	13.0	22.5	—	41.8	7.62

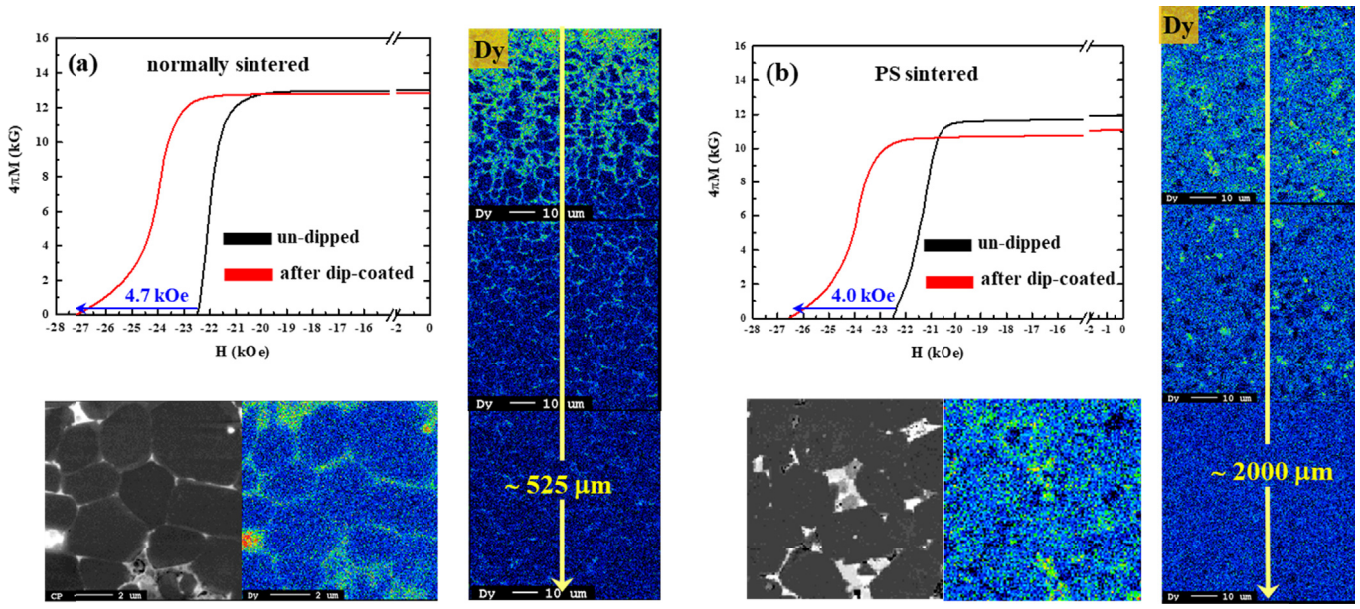

Fig. 4. Comparison of demagnetization behavior and Dy penetration depth between (a) the normally sintered magnet and (b) the PS sintered magnet. Both samples were GBD treated with DyH_2 + Al solution

(4.7 kOe). To figure out why the PS sintered GBDP magnet exhibited such smaller increase of ${}_iH_c$ in-spite of the remarkable increase of Dy penetration, TEM investigation was performed as shown in Fig. 5 & 6.

As shown in Fig. 5, thin grain boundaries are connected with Nd-rich triple junctions in a NdFeB sintered magnet. In order to ensure high coercivity, magnetic grains in the magnet should be decoupled well by a thin nonmagnetic Nd-rich grain boundary phase that encloses individual grain. Some grain boundaries in the PS sintered GBDP magnet were developed well as typically shown in Fig. 5 (2), filled with Nd-rich phase, but others were not developed well thereby the decoupling of the grains was incomplete (Fig. 5 (1)). The Nd-rich phase in the grain boundary is permeated from the Nd-rich triple junc-

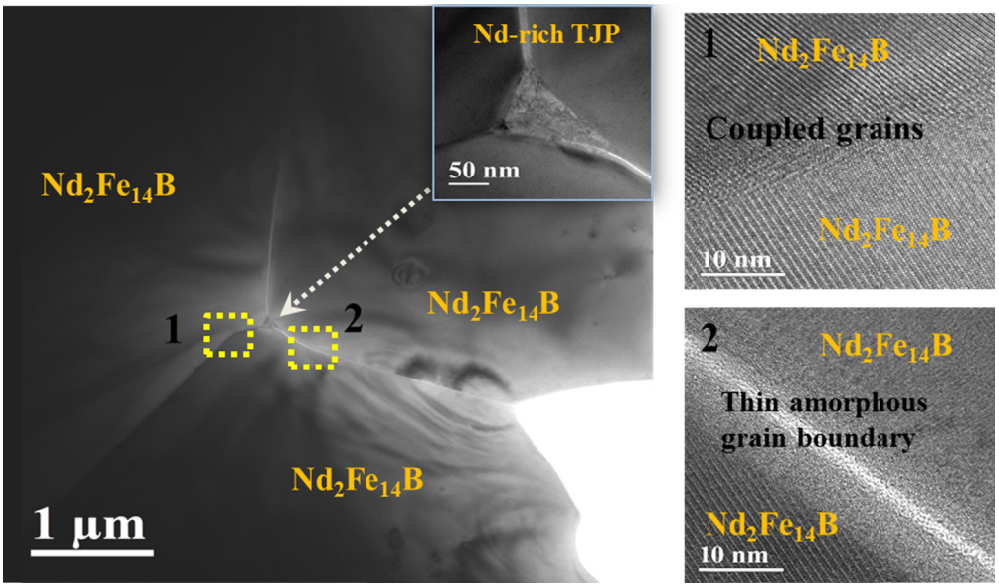

Fig. 5. High resolution TEM micrographs of grain boundary area in a PS sintered magnet GBD treated with DyH_2 + Al solution

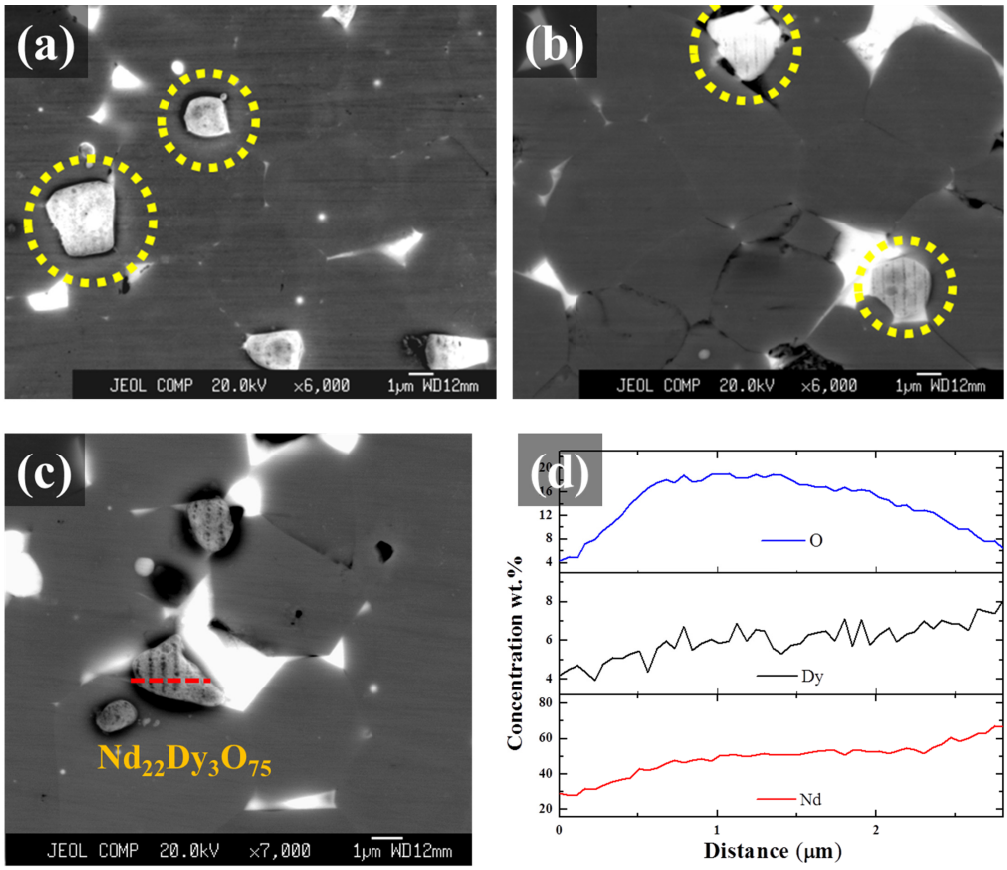

Fig. 6. TEM micrographs of the PS sintered magnets GBD treated with (a) DyH_2 + Al and (b) DyH_2 + Cu solution. Lamella-structured oxide phases found in both (a) and (b) are shown and analyzed in detail in (c) and (d), respectively

tion region [14,15]. If the entrance of the grain boundary from the triple junction is blocked by an oxide, as can be seen in the figure, or oxygen content of a magnet is high, the Nd-rich grain boundary phase is not developed continuously during annealing because the melting temperature of the Nd-rich phase increases [14,15]. In fact, the oxygen content in the normally sintered magnet was about 3,000 ppm whereas that in the PS sintered magnet increased to about 6,200 ppm, and increased further after GBDP to 6,900 ppm. Considerable amount of oxygen was obviously introduced to the magnet during preparation for PS sintering and dipping which had to be done in the air in this experiment. Therefore, aforementioned smaller increase of $_iH_c$ in the PS sintered GBDP magnet was attributed to such a high oxygen content that subsequently induced the formation of many oxides as can be found in Fig. 6.

As shown in Fig. 6, many oxide phases (circled area) were existed mostly in the triple junction region in the PS sintered GBDP magnets treated both with Al and Cu mixed DyH_2 solution. Some of them had lamellar structure like the one in Fig. 6(c), and these oxides were found to be Dy contained Nd oxides (Fig. 6(d)). It was found that, in (Dy,Nd)-Fe-B sintered magnet, the Dy atoms not only substituted for Nd atoms in the $Nd_2Fe_{14}B$ main phase, but also formed their own oxide phases in the triple junction regions [16]. Accordingly, in the PS sintered GBDP magnet with high oxygen content, the Dy atoms were largely consumed to form (Dy,Nd)-O phase in the triple junction region and only the rest of them would be used for substitution of Nd in $Nd_2Fe_{14}B$ grains to make core-shell type structure although the Dy atoms penetrated deeper inside the magnet (As in Fig. 4(b)), resulting in smaller increase of $_iH_c$ by GBDP. This is also responsible for further decrease of B_r in the PS sintered GBDP magnet. The enclosed process system used in Ref.[17] would be helpful to prevent the introduction of excessive oxygen to the PS sintered GBDP magnets and bring about better magnetic properties.

4. Conclusions

The pre-sintering process adopted for making a GBDP magnet apparently improved the diffusivity of Dy atoms through grain boundaries. The penetration of Dy into the magnet extended almost to 2,000 μm from the surface, about four times deeper than that of the normally sintered and GBD treated one, when the DyH_2 + Al solution was used as a Dy source. However, the resulting increase of coercivity is about 4 kOe, somewhat lower than that of the normally treated one, mostly due to excessive formation of Dy-contained oxides that hindered to make a thin continuous Nd-rich grain boundary phase and a core-shell type structure. Therefore, to utilize the pre-sintering process for high coercivity HRE saving magnets, one should find the way to prevent excessive inflow of oxygen during the entire process, for instance, using a closed process system.

Acknowledgments

This work is supported by the Sun Moon University Research Grant in 2018.

REFERENCES

[1] K.H.J. Buschow, J. Mater. Sci. Res. **1**, 1 (1986).
[2] J.F. Herst, Rev. Mod. Phys. **63**, 819 (1991).
[3] J. Fidler, J. Bernardi, J. Appl. Phys. **70**, 6456 (1991).
[4] W.F. Li, T. Ohkubo, K. Hono, M. Sagawa, J. Magn. Magn. Mater. **321**, 1100 (2009).
[5] T.S. Jang, Trends in Metals & Mat. Eng. (Korean) **23** (2), 24 (2010).
[6] K. Hirota, H. Nakamura, T. Minowa, M. Honshima, IEEE Trans. Magn. **41**, 2909 (2006).
[7] D.S. Li, M. Nishimoto, S. Suzuki, K. Nishiyama, M. Itoh, K. Machida, 2009 IOP Conf. Ser.: Mater. Sci. Eng. **1**, 012020 (2009).
[8] M. Komuro, Y. Satsu, H. Suzuki, IEEE Trans. Magn. **46**, 3831 (2010).
[9] Y. Takata, K. Fukumoto, Y. Kaneko, A. Manabe, N. Miyamoto, S. Imada, S. Suga, J. Jpn. Soc. Powder Metallurgy **57** (12), 789 (2010).
[10] M.W. Lee, T.S. Jang, J. Koran Powder Metall. Inst. (Korean) **23** (6), 432 (2016).
[11] K.H.J. Buschow, Handbook of Magnetic Materials **10**, 512 (1997).
[12] M.W. Lee, K.H. Bae, S.R. Lee, H.J. Kim, T.S. Jang, Arch. Metall. Mater. **62** 2B, 1263 (2017).
[13] Junjie Ni, Tianyu Ma, Mi Yan, J. Magn. Magn. Mater. **323**, 2549 (2011).
[14] K.H. Bae, S.R. Lee, H.J. Kim, M.W. Lee, T.S. Jang, J. Appl. Phys. **118**, 203902 (2015).
[15] W.F. Li, T. Ohkubo, K. Hono, Acta Materialia **57**, 1337 (2009).
[16] W.F. Li, H. Seperi-Amin, T. Ohkubo, N. Hase, K. Hono, Acta Materialia **59**, 3061 (2011).
[17] M. Sagawa, Proc. 21st Workshop on Rare-Earth Permanent Magnets and their Applications, 183 (2010).